



DESIGN OF A UWB WIRELESS INDOOR RAKE RECEIVER USING CONTINUOUS AND DISCRETE WAVELET TRANSFORM APPROACHES

¹RASHID A. FAYADH, ²F. MALEK, ³HILAL A. FADHIL, ⁴SAMEER K. SALIH, AND ⁵FARRAH SALWANI ABDULLAH

¹Ph.D Student, School of Computer and Communication Engineering, University Malaysia Perlis, Malaysia

²Assoc. Prof., School of Electrical Systems Engineering, University Malaysia Perlis, Malaysia

³Dr., School of Computer and Communication Engineering, University Malaysia Perlis, Malaysia

⁴Ph.D Student, School of Computer and Communication Engineering, University Malaysia Perlis, Malaysia

⁵Dr., School of Electrical Systems Engineering, University Malaysia Perlis, Malaysia

E-mail: r_rashid47@yahoo.com, mfareq@unimap.edu.my, hilaladnan@unimap.edu.my,
sameerksalih@yahoo.com, farrahsalwani@unimap.edu.com

ABSTRACT

In this paper, four levels of analysis and synthesis filter banks are proposed to create, coefficients for a continuous wavelet transform (CWT), a discrete wavelet transform (DWT), and an inverse, discrete wavelet transform (IDWT). The main property of these wavelet transform schemes is their ability to construct the transmitted signal across a log-normal fading channel over additive, white Gaussian noise (AWGN). There are many applications of wavelet transforms in wireless communication systems, and we chose the design of rake receivers as a major application to mitigate interferences and reduce the noise. In this research, a new scheme of rake receivers was proposed to receive indoor, multi-path components (MPCs) for ultra-wideband (UWB) wireless communication systems. Rake receivers consist of a continuous wavelet rake (CWR) and a discrete wavelet rake (DWR), and they use huge bandwidth (7.5 GHz), as reported by the Federal Communications Commission (FCC). The indoor channel models chosen for analysis in this research were the line-of-sight (LOS) channel model (CM1 from 0 to 4 meters) and the non-line-of-sight (NLOS) channel model (CM3 from 4 to 10 meters). Two types of rake receiver were used in the simulation, i.e., partial-rake and selective-rake receivers with the maximal ratio combining (MRC) technique to capture the energy of the signal from the output of the rake's fingers. In the simulation, the transmitted and received radiations are presented with UWB single-in, single-out (SISO) with Walsh matrix coding.

Keywords: *UWB Indoor Wireless Communication Systems, LOS And NLOS Channel Models, Continuous Wavelet And Discrete Wavelet Rake Receivers, Analysis And Synthesis Filter Banks.*

1. INTRODUCTION

The UWB wireless communication system is a technology that uses short pulses (ns) for the transmission and reception of data, so it is suitable for high-speed, wireless, indoor systems [1, 17]. According to reports provided by the FCC, the UWB of 7.5 GHz, ranging from 3.1 GHz- to 10.6 GHz as shown in Figure 1, spreads the energy of the pulse across this 7.5 GHz wideband [2]. The transmission power's spectral density (PSD) is low (-41.3 dBm/MHz), therefore it decays easily in a short time and over short ranges [3]. A rake receiver with several fingers was designed to collect copies of the resolvable, multi-path components (MPCs) that were received as a supporting technique for

capturing most of the signal's energy [4]. Many papers have been published on rake receivers with channel estimation, and they have used different techniques for combining signals with the three main types of rake receivers, i.e., all rake (A-rake), selective rake (S-rake), and partial rake (P-rake) [5, 6]. Recently, the wavelet transform scenario has been used in the UWB communication field to analyze and synthesize the UWB signal in order to construct the desired signal from the background noise [7, 27] and was used to detect the breast cancer [21]. The wavelet transform (WT) technique is a modern area of mathematics that is applied for compressing signals and images and removing noise from their coefficients [8, 22]. The signal-to-noise ratio (SNR) can be improved by using a WT

approach that decomposes the signal into different scales and different levels of resolution. Wavelet video compression was evaluated and achieved in [9], [29] for wideband, multi-carrier, code-division, multiple access (MC-CDMA) and a rake receiver over additive, white Gaussian noise (AWGN) and the Rayleigh fading channel. A novel wavelet rake receiver (WR) based on continuous wavelet transform (CWT) was presented in [10], and it showed a great enhancement in performance with a less complex receiver. The proposed CWT and DWT rake receivers were designed with CWT and DWT template references of the transmitted pulse at different scales and different frequency centers. These receivers depend on the algorithm for wavelet signal decomposition that converts the signal to four levels to produce the approximated and detailed coefficients.

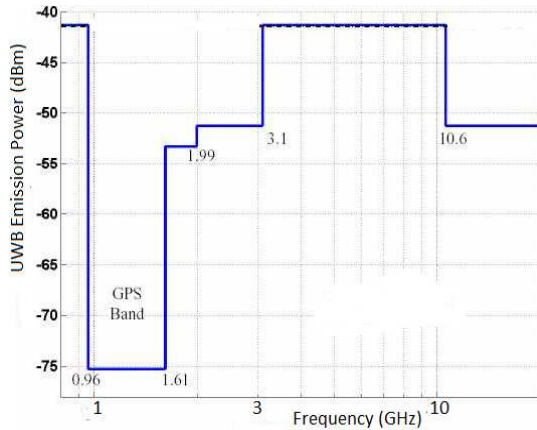


Figure 1: FCC-UWB Spectrum Corresponding To Wireless Indoor Propagation

The remainder of the paper is organized as follows. Section 2 addresses UWB transmission signals and channel models. Section 3 presents a brief discussion of wavelets transform (WT) and continuous wavelets transform (CWT). Section 4 introduces four levels of discrete wavelet transforms (DWTs) for analysis and synthesis processing. Section 5 presents the structures of CWR and DWR rake receivers. The simulation results are presented and discussed in section 6, and our conclusions are given in section 7 while the acknowledgment is produced in section 8.

2. TIME-HOPPING, SPREAD-SPECTRUM, ULTRA WIDEBAND (THSS-UWB) SCHEME

We considered the transmitted pulse trains that are modulated by the binary-phase, shift-keying (BPSK), modulation technique that represents bit 1

for a positive-polarity pulse and bit 0 for a negative-polarity pulse. The M-array BPSK signal $X(t)$ and transmitted signal $S(t)$ are defined as [11]:

$$X(t) = \sum_{p=-\infty}^{\infty} d_p G_2(t - pT_f) \quad (1)$$

$$S(t) = \sum_{p=-\infty}^{\infty} G_2(t - pT_f - c_p T_c - m_p T_d) \quad (2)$$

where G_2 is the second derivative Gaussian pulse that is transmitted as shown in Figure 2 in the time and frequency domains, T_c is the chip duration, T_f is the frame duration, $d_p \in \{-1, +1\}$ is a bit stream, c_p is the p -th integer value of the pseudo-random code from 0 to $N-1$, and it is assumed that $NT_c \leq T_f$. Each transmitted bit with a number of pulses (N_s) has a duration of $T_s = N_s T_f$ of time division for the TDSS-UWB characteristic, as shown in Figure 3.

In indoor multipath propagation, the Saleh-Valenzuela (S-V) model [12] provides two channel models, i.e., CM1 for a range of 0 to 4 m and CM3 for a range of 4 to 10 m. The parameters of the models are defined in Table 1, and they were used in MATLAB simulation with a log-normal distribution [13]. The channel impulse response $h(t)$ for each of these models can be modeled by

$$h(t) = \sum_{k=0}^{K-1} \sum_{l=0}^{L-1} \alpha_{k,l} \delta(t - T_c - \tau_{k,l}) \quad (3)$$

where $\alpha_{k,l}$ is the channel gain of the l th multipath component in the k -th cluster, K is the total number of clusters, L is the total number of rays in each cluster, δ is the dirac function, and $\tau_{k,l}$ is the delay of l -th ray within each cluster.

For the receiving signal $r(t)$ model, we consider one user with a total energy that is equal to 1. The noisy signal that is received consists of the signal transmitted by the user $S(t)$ and the adaptive, white, Gaussian noise (AWGN) $n(t)$ of zero mean and two-sided power spectral density $N_0/2$, which can be written as:

$$r(t) = S(t) * h(t) + n(t) \quad (4)$$

$$r(t) = \sum_{k=0}^{K-1} \sum_{l=0}^{L-1} \alpha_{k,l} S(t - T_l - \tau_{k,l}) + n(t) \quad (5)$$

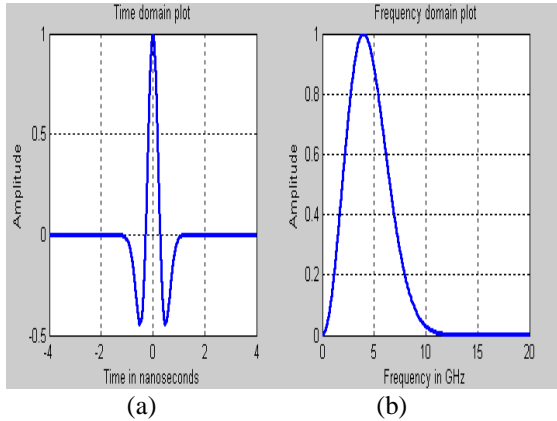


Figure 2: Second Derivative Gaussian Pulse In (A) The Time Domain And (B) The Frequency Domain

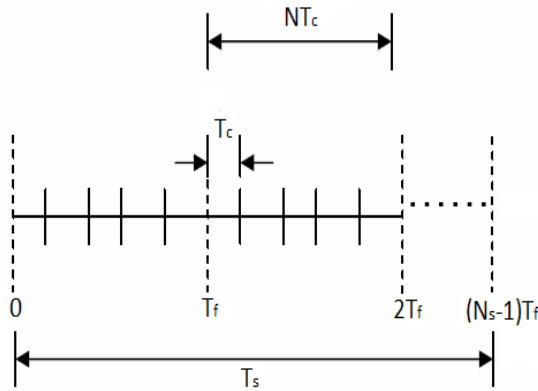


Figure 3: Thss-Uwb Scheme

3. WAVELET TRANSFORM

The wavelet transform technique is a mathematically-suitable tool that makes the wavelet properties useful for signal processing by converting the signal into a series of wavelets [30]. The information can be extracted from many kinds of data by using multi-resolution analysis in both the frequency and time domains at different scales. In order to be more flexible in extracting time and frequency information, there is a function called the mother wavelet (MW) function, $\psi(t)$, that was derived with continuous scaling and shift parameters, a and b , respectively [14, 19, 20, 24].

$$\psi_{a,b}(t) = \frac{1}{\sqrt{a}} \psi\left(\frac{t-b}{a}\right) \quad (6)$$

To analyze the signal on the wavelet function, multiplication and integration must be implemented using MW to change the size of the analysis function to get more resolution [15].

$$\langle S(t), \psi_{a,b}(t) \rangle = \int_{-\infty}^{\infty} S(t) \psi_{a,b}(t) dt \quad (7)$$

The continuous time wavelet transform (CWT), $G_l(a,b)$, of the received continuous-time transmitted pulse $S(t)$ can be expressed as:

$$G_l(a,b) = \int_{-\infty}^{\infty} \frac{1}{\sqrt{a}} S(t) \psi^*\left(\frac{t-b}{a}\right) dt \quad (8)$$

where ψ^* is the complex conjugate of function and the signal is expanded when scale $a > 1$ and compressed when scale $a < 1$. The CWT is regarded as the inner product of the signal $r(t)$ with a basis function $\psi^*_{a,b}(t)$, and it represents the same signal, but with different frequency bands and different frequency centers (f_c) for each existing band at what time interval. These bands (B_s), which have better time localization, are shown in Figure 4 to make a wavelet transform that is suited for most signal and image applications, so that B_2 is double B_1 , B_3 is double B_2 , and B_4 is double B_3 . The inverse wavelet transform (IWT) can be expressed as shown below:

$$S(t) = \frac{1}{C_\psi} \int_0^\infty \int_{-\infty}^\infty W_s(a,b) a^{-\frac{1}{2}} \psi\left(\frac{t-b}{a}\right) db \frac{da}{a^2} \quad (9)$$

and C_ψ is defined as:

$$C_\psi = \int_0^\infty \frac{|\Psi(\omega)|^2}{\omega} d\omega, \quad (10)$$

where C_ψ is the Fourier transform of MW(t) and also is called the admissibility condition.

Table 1: Channel Model Parameters Provided by the FCC

Channel Parameters	CM1	CM3
	(LOS 0-4 m)	(NLOS 4-10 m)
Λ (1/ns)- cluster arrival rate	0.0233	0.0667
λ (1/ns) -ray arrival rate	2.5	2.1
Γ - cluster decay factor	7.1	14.00
γ -ray decay factor	4.3	7.9
σ_1 - standard deviation of cluster lognormal fading term (dB).	3.3941	3.3941
σ_2 -standard deviation of ray lognormal fading term (dB)	3.3941	3.3941
σ_x - standard deviation of lognormal shadowing term for total multipath realization (dB).	3	3

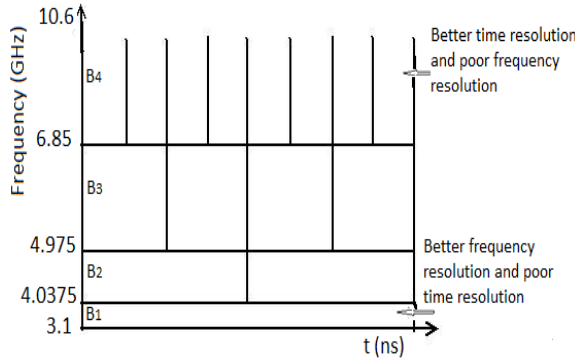


Figure 4: Time-Frequency Representation of the UWB Wavelet Transform

4. DISCRETE WAVELET TRANSFORM (DWT)

The DWT is used to provide adequate information during the analysis and synthesis process while decreasing the computation time required [25]. The implementation of DWT consists of filters of different cutoff frequencies that are used to analyze the signal at different scales (high-pass filters to analyze high frequencies and low-pass filters to analyze low frequencies). These filters operate to enhance the resolution of the signal by changing the scale by a factor j to obtain sub-sampling by reducing the sampling rate or

removing some of the sample signal [28]. Since the signal is a discrete time function with a sequence that is denoted by $r[j]$ (j is an integer), the convolution operation is defined as follows [16, 18, 23]:

$$h[j] = \sum_{i=-\infty}^{\infty} r[j].h[j-i] \quad (11)$$

$$r[j]*g[j] = \sum_{i=-\infty}^{\infty} r[j].g[j-i], \quad (12)$$

where $h[j]$ is the impulse response of the half band low-pass filter and $g[j]$ is the impulse response of the half band high-pass digital filter. The DWT coefficients are sampled from CWT as shown in Figure 5 by an algorithm, which is called the sub-band, coding algorithm, to sub-sample the output signal $Y[j]$ from each filter by two (divide by two) and they are mathematically expressed as:

$$Y_{high}[i] = \sum_j r[j].g[2i-j] \quad (13)$$

$$Y_{low}[i] = \sum_j r[j].h[2i-j], \quad (14)$$

where, $Y_{high}[I]$ and $Y_{low}[I]$ are the outputs of the high-pass and low-pass filters, respectively. As shown in Figure 6, the reconstruction or inverse discrete wavelet transform (IDWT) to signal $r[j]$ is a process that consists of up sampling ($\uparrow 2$) and reconstruction or inverse discrete wavelet transform (IDWT) filtering that can be done depending on the relationship between the impulse responses of the low-pass and high-pass filters by the following related expressions:

$$g[D-1-j] = (-1)^j.h[j] \quad (15)$$

$$r[j] = \sum_{i=-\infty}^{\infty} (Y_{high}[i].g[-j+2i]) + (Y_{low}[i].h[-j+2i]) \quad (16)$$

where D is the length of the filter (number of points) and $(-1)^j$ is a term that provides conversion from low-pass to high-pass.

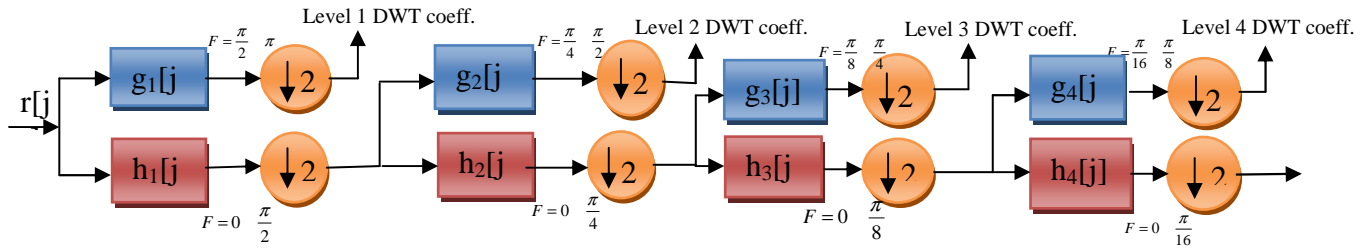


Figure 5: Analysis Filter Bank for the Sub-Band Coding Algorithm to Create DWT Coefficients

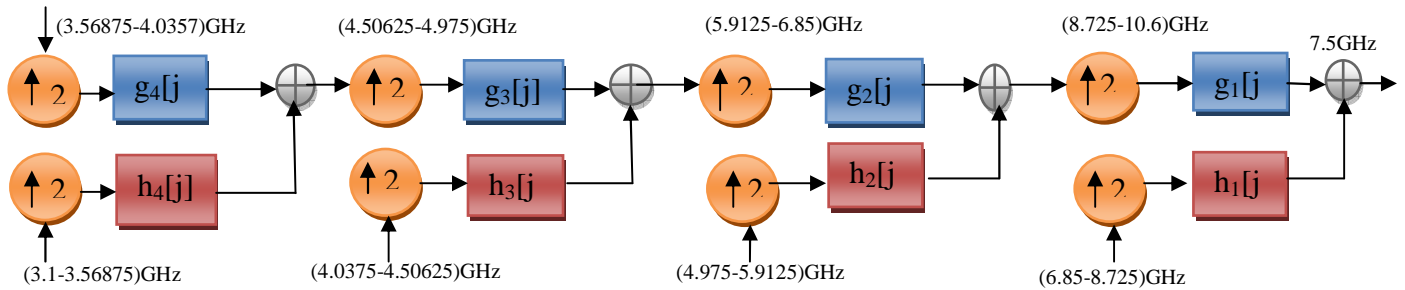


Figure 6: Synthesis Filter Bank for Computing IDWT Coefficients

5. THE PROPOSAL DESIGN FOR CONTINUOUS WAVELET RAKE (CWR) AND DISCRETE WAVELET RAKE (DWR) RECEIVERS

The proposed rake receivers consist of several correlators (fingers) followed by a maximal ratio combiner (MRC) that combines the outputs of the fingers. The types of rake receivers were assumed to be partial and selective rake receivers, which select the first non-zero arriving paths (L_p) and the strongest propagation arriving paths (L_s), respectively. In the CWR and DWR receivers that are shown in Figure 7 and Figure 8, respectively, the template waveforms are CWT (G_{al}) of the transmitted pulse $G_2(t)$ at different center frequencies (F_{cl}) and different scales (a_l) of the l th rake correlators ($l = 0 \dots L-1$). These template signals are highly correlated with the transmitted pulse, and they are separated by the τ_{gl} that matches the center frequency [26]. The output mathematical expression for each correlator over the frame duration is:

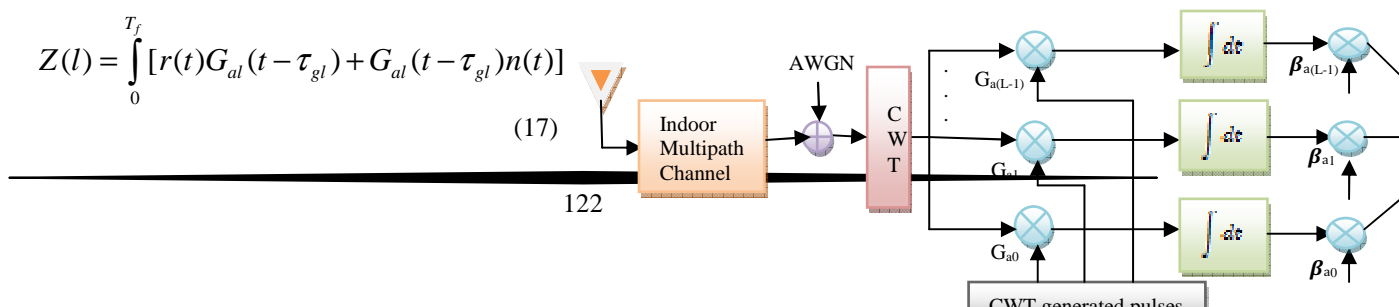
$$Z(l) = \int_0^{T_f} [r(t)G_{al}(t - \tau_{gl}) + G_{al}(t - \tau_{gl})n(t)] \quad (17)$$

Since the proposed rake receiver uses MRC to maximize the SNR, the total output signal (Y_{tot}) of the combiner for the first arriving paths (L_p) and selective paths (L_s) can be written as:

$$Y_{tot.} = \sum_{L_p=0}^{L_p-1} Z(l)\beta_{al} \quad (18)$$

$$Y_{tot.} = \sum_{L_s=0}^{L_s-1} Z(l)\beta_{al}, \quad (19)$$

where β_{al} is the gain factor for the l^{th} finger under the condition $\sum_{l=0}^{L-1} \beta_{al} = 1$



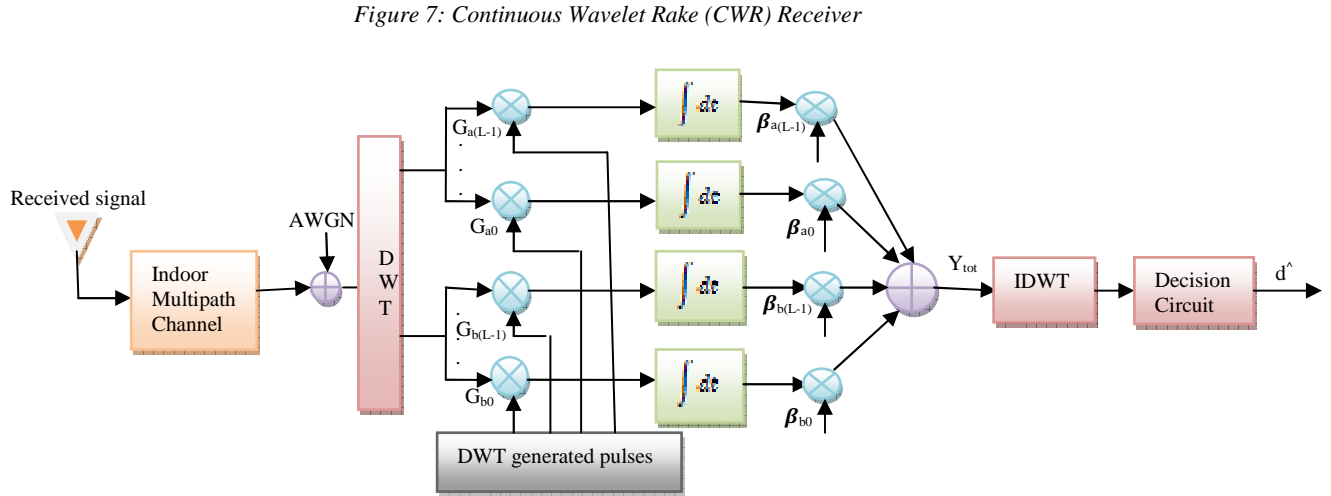


Figure 7: Continuous Wavelet Rake (CWR) Receiver

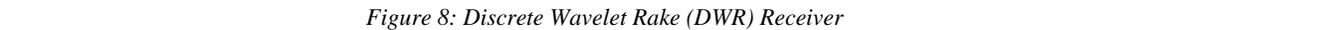


Figure 8: Discrete Wavelet Rake (DWR) Receiver

6. SIMULATION RESULTS AND DISCUSSION

One thousand random bits are generated in the transmitter, and they use PPM for modulation. The spreading factor is 16, and the data are coded by the Walsh matrix. The encoded pulses are added to AWGN and the noisy signal, as shown in Figure 9, and the combined signal and pulses pass through multi-path (50 paths), log-normal, fading channels (CM1 of LOS and CM3 of NLOS). First, the noisy signal is supplied to the CWT rake receiver of the template of the continuous wavelet transform signal with four levels of significance in order to operate with the data stream of information. MATLAB simulation was used to simulate the four levels of filters with partial and selective rake receivers of the MRC combiner over AWGN and log-normal fading channels. The wavelet decomposition structure of the Coiflet3 filter (IIR filter with three coefficients) was used to reconstruct an approximation of the signals and the detailed signals at levels 1 to 4 composed of scales 2, 4, 8, and 16. From Figure 10 and Figure 11, an

approximation of the signals and the detailed signals are shown for CM1 and CM3 to denote the amount of noise that can be canceled in order to construct the desired signal.

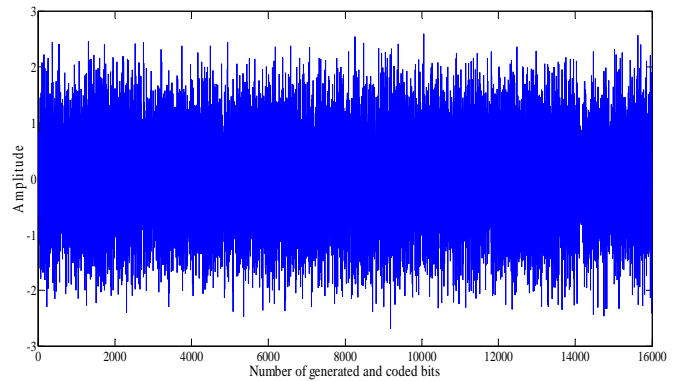


Figure 9: Encoded, Noisy, As-Received Data Stream

Figure 12 shows the results of the four decomposition levels using CM1, and Figure 13 shows the results using CM3 and the FCC channel parameters in Table 1, i.e., (a) level 1 to extract the approximate and detailed coefficients from the original received signal as shown in Figure 9, (b) level 2 produces new approximate and detailed

coefficients from the signal of level 1, and (c) level 3 shows the expressing coefficients of the signal from level 2, and level 4 reads out the coefficients of the signal from level 3. So, from these results, the design of the filter bank of the three levels in a discrete wavelet transform is sufficient to minimize noise and interference.

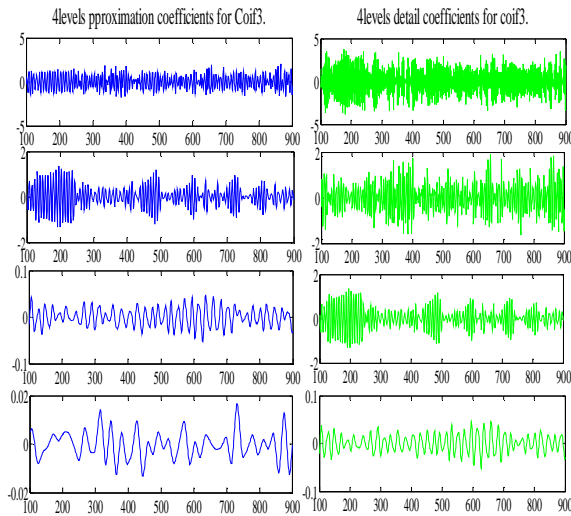


Figure 10: CWT 4 Levels Of Decomposition Using CM1

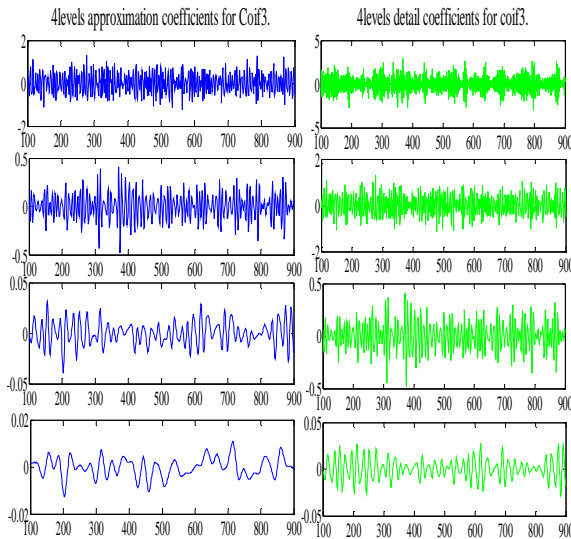


Figure 11: CWT4 Levels Of Decomposition Using CM3

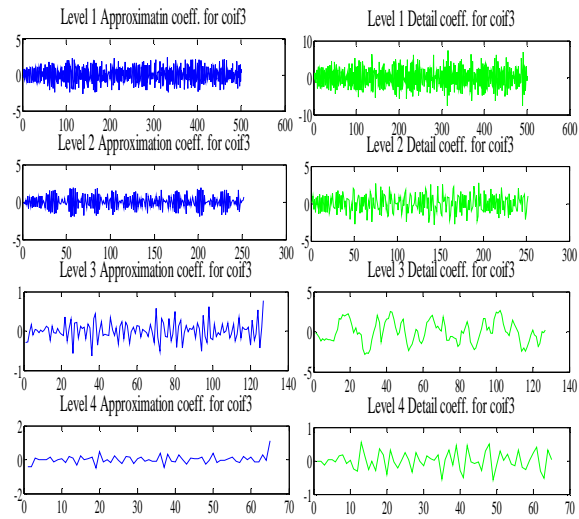


Figure 12: DWT 4 Levels Decomposition Using CM1

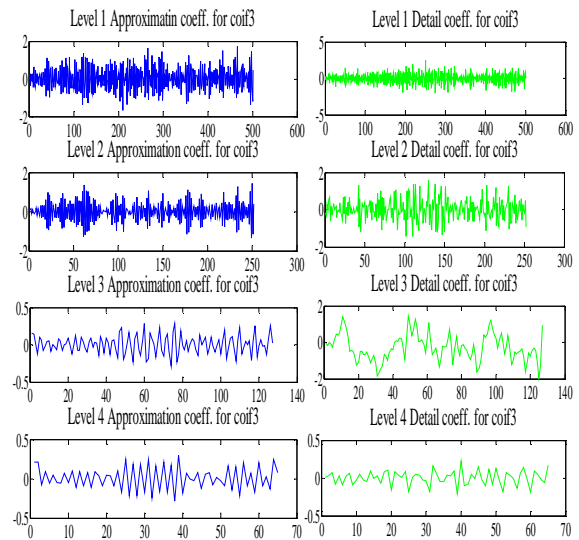


Figure 13: DWT 4 Levels Decomposition Using CM3

In the simulation process, four rake fingers were chosen in both receivers, i.e., $L_p = 4$ and $L_s = 4$, and two users also were chosen. Figure 14 shows the performance of the partial and selective continuous wavelet rake receivers (P-CW-rake and S-CW-rake) with the conventional partial and selective rake receivers (C-P-rake and C-S-rake) for the multi-path channel model CM1. The goal of using these proposed receivers is to reduce the BER in comparison with conventional rake receivers, at 8 dB SNR, The BER decreases from 0.1668 in C-P-

rake to 0.00218 in P-CW-rake and from 0.0645 in C-S-rake to 0.00067 in S-CW-rake. Figure 15 shows BER versus SNR with multi-path CM1 channel model parameters to display the behavior of the BER for different values of SNR using partial and selective discrete wavelet rake receivers (P-DW-rake and S-DW-rake). The simulation results indicated that the S-DW-rake receiver outperformed the P-DW-rake receiver in reducing the BER, because it used the strongest paths for selecting the MPCs. The efficiencies of these proposed receivers were compared with those of conventional rake receivers (C-P-rake and C-S-rake) through LOS channel conditions. In 8 dB SNR, the value of the BER reduces from 0.1959 in C-P-rake to 0.0004 in P-DW-rake and from 0.1600 in C-S-rake to 0.0007 in S-DW-rake receivers. In order to determine the advantage of using DW-rake receiver instead of CW-rake receiver, for example, at a BER of 10⁻³, the SNR is 13dB for P-CW-rake, 4.5dB for P-DW-rake, 6.3dB for S-CW-rake, and 1.8dB for S-DW-rake. So that, the advantages are presented about 8.5 dB with respect to partial combining strategy and 4.5 dB with respect to selective combining strategy.

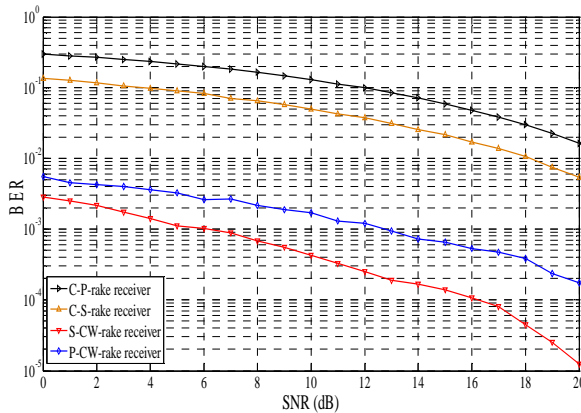


Figure 14: Scenario for BER Performance in the CWR Scheme of CM1 with Four Fingers and Two Users

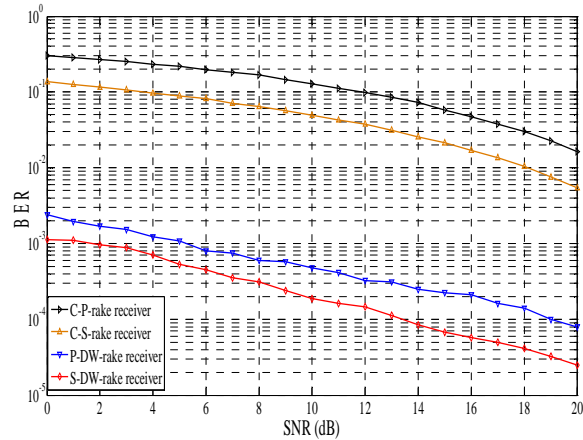


Figure 15: Scenario for BER Performance in the DWR Scheme of CM1 with Four Fingers and Two Users

For a multi-path, NLOS, channel model CM3 with a range of 10 m with the parameters presented in Table I of the FCC report, Figure 16 shows that the BER was minimized for the partial-rake and selective-rake CW-rake receivers. The BER was 0.2 for the C-P-rake and 0.17 for C-S-rake selective-rake receiver at an SNR of 8 dB, these values are reduced to be 0.00176 and 0.00097 for the P-CW-rake and S-CW-rake, respectively. Figure 17 shows the enhanced performance of the P-DW-rake and S-DW-rake over the P-CW-rake and S-CW-rake receivers. At an SNR of 8 dB, the BER of the partial rake receiver was reduced from 0.1668 with C-P-rake to 0.0006 with P-DW-rake and from 0.0644 with C-S-rake to 0.00031 with S-DW-rake. To calculate the gains of using DW-rake over CW-rake receivers, for example, at a BER of 10⁻³, the SNR is 10.8dB for P-CW-rake, 6.2 dB for S-CW-rake, 7.8 dB for P-DW-rake, and 2.3 dB for S-DW-rake. The gains are 4.6dB for partial rake receiver and 5.5 dB for selective rake receiver. From simulation results in Figures 14, 15, 16, and 17, as expected, the selective rake strategy has better performances than the partial rake strategy in both presented CW-rake and DW-rake receivers over CM1 and CM3 channel model parameters.

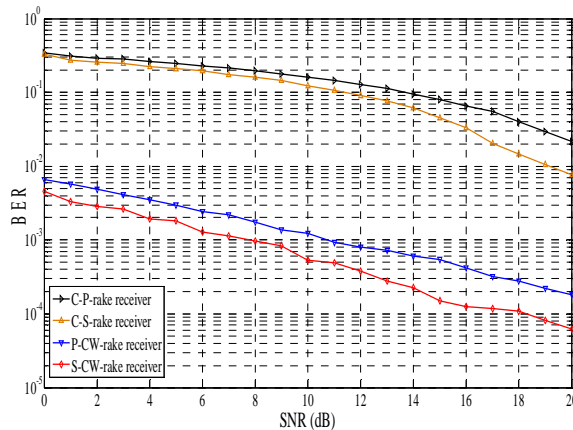


Figure 16: Scenario for the BER Performance in the CWR Scheme of CM3 with Four Fingers and Two Users

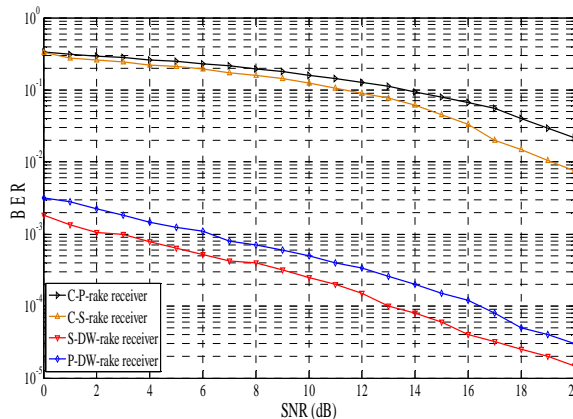


Figure 17: Scenario for the BER Performance in the DWR Scheme of CM3 with Four Fingers and Two Users

7. CONCLUSINS

Performance analysis and synthesis of the filter banks for continuous wavelet transform and discrete wavelet transform were investigated for four levels. The approximate and detailed coefficients were determined and compared with the original, noisy signal that was received. From the output of each level, we were able to determine how many levels had to be used in the design to construct the desired signal. In the simulation, we used three levels of the filter bank scheme (up to the third level) in the proposed CW-rake and DW-rake receivers to determine the bit-error probability (P_e) at different values of SNR. The designed partial-rake and selective-rake receivers were evaluated with four fingers for the CM1 and CM3 channel models. The performances of the partial and selective CW-rake and DW-rake receivers were compared with that of a conventional rake receiver,

and, in a agreement with the simulation results, it was observed that the BER was decreased at low SNR values. By using the two proposed receivers, we reduced the probability of error in constructing the desired signal for the decision circuit of the rake receiver was executed by these proposed receivers. The results of our research confirmed the performance enhancement that resulted from the use of the two proposed receivers in that there was a high correlation between the transmitted signal and the wavelet signal, and there was a poor correlation with the noise signal.

ACKNOWLEDGMENT

The authors would like to sincerely thank Dr. Mohd Farek Abd Malek for his thoutful comments on this paper. Special thanks to University Malaysia Perlis.

REFERENCES:

- [1] Oppermann et al., "UWB Theory and Applications," *John Wiley*, 2004.
- [2] F. Nekoogar, "Ultra Wideband Communications: Fundamentals and Application," *Prentice Hall*, Dec. 2004.
- [3] D. Tse and P. Viswanath, "Fundamentals of Wireless Communication," *Cambridge University Press*, 2005.
- [4] D. Cassioli, M. Z. Win et al., "Low Complexity Rake Receivers in Ultra-Wideband Channels," *IEEE Trans. Wireless Communications*, vol. 6, no. 4, Apr. 2007, pp. 1265-1275.
- [5] M. Z. Win, D. Dardari, A. F. Molish et al., "History and Applications of UWB," *Proceedings of the IEEE*, vol. 97, no. 2, Feb. 2009, pp. 198-204.
- [6] Q. Z. Ahmed and L. L. Yang, "Reduced-Rank Adaptive Multiuser Detection in Hybrid Direct-Sequence Time-Hopping Ultrawide Bandwidth Systems," *IEEE Trans. Wireless Communications*, vol. 9, no. 1, Jan. 2010, pp. 156-167.
- [7] Lloyd Emmanuel, Xavier N. Fernando "Wavelet-Based Spectral Shaping of UWB Radio Signal for Multisystem Coexistence," *Computers and Electrical Engineering Journal*, vol. 36, no. 2, Mar. 2010.
- [8] D. L. Donoho and I. M. Johnstone, "Ideal spatial adaptation by wavelet *Shrinkage*," *Biometrika*, vol. 81, no. 3, 1994, pp. 425- 455.



- [9] Minh Hung Le and Nikos E. Mastorakis, "Performance Analysis of Wideband MC-CDMA for Wavelet Vidio with Multilevel UEP Code over Fading Channels," *5th WSEAS INT Conf. Corfu, Greece, Aug. 2005*, pp 114-119.
- [10] Amara I. Zaki, Said E. El-Khamy and Ehab F. Badran, "A Novel Rake Receiver Based on continuous Wavelet Transform Designed for UWB Systems," *European Journal of Scientific Research*, Vol. 83, No.4, 2012, pp 463-474.
- [11] Nikoogar H., and Prasad R., "Introduction to ultra wideband for wireless communications," *Berlin, Springer*, ISBN 978-1- 4020-6632-0 , 2009.
- [12] Adel M. Saleh and Reinaldo A. Valenzuela, "A Statistical Model for Indoor Multipath Propagation," *IEEE Journal on Selected Areas in Communication*, Vol. SAC-5, No. 2, Feb. 1987.
- [13] Jeff Foerster, Intel R & D, "Channel Modeling Sub-Committee Report Final," IEEE p802.15-02/490r1-SG3a, Aug. 2012.
- [14] Ali A. A. , "Discrete Wavelet Transform Based Wireless Digital Communication," *Discrete Wavelet Transforms-Theory and Application*, Dr. Juuso T. Olkkonen (Ed.), Apr. 2011.
- [15] Ioana Adam, "Complex Wavelet Transform:application to denoising," PhD. Thesis, Politehnica University of Timisoara, 2011.
- [16] Ali N. Akansu, Wouter A. Serdijn, Ivan W. Selesnick, "Emerging Applications of Wavelets: A Review," *Physical Communication Journal*, vol. 3, no. 1, 2010.
- [17] Savo G. Glisic, "Advanced Wireless Networks 4G Technologies," *John Wiley & Sons Ltd*, The Atrium, Southern Gate, Chichester, West Sussex PO19 8SQ, England, 2006.
- [18] M. K. Lakshmanan and H. Nikoogar, "A Review of Wavelets for Digital Wireless Communication," Springer, *Wireless Personal Communications*, No. 37, 2006, pp. 387-420.
- [19] M. Sifuzzaman, M.R. Islam and M.Z. Ali, "Application of Wavelet Transform and its Advantages Compared to Fourier Transform," *Journal of Physical Sciences*, Vol. 13, 2009, pp. 121-134.
- [20] Martin Vetterli and Jelena Kovačević, "Wavelets and Sub-band Coding," *Second Edition, Prentice Hall PTR*, Englewood Cliffs, New Jersey, 2007.
- [21] B. McGinley, M. O'Halloran, R. Conceicao, G. Higgins, E. Jones, and M. Glavin, "The Effect of Compression on Ultra Wide-Band Radar Signal," *Progress In Electromagnetic Research*, Vol. 117, 2011, pp. 51-65.
- [22] Mahboob Iqbal, Jie Chen, Wei Yang, Pengbo Wang, and Bing Sun, "SAR Image Despeckling by Selective 3D Filtering of Multiple Compressive Reconstruction Images," *Progress In Electromagnetic Research*, Vol. 134, 2013, pp. 209-226.
- [23] Y. Zhang and L. Wu, "An Mr Brain Images Classifier Via Principal Component Analysis and Kernel Support Vector Machine," *Progress In Electromagnetic Research*, Vol. 130, 2012, pp. 369-388.
- [24] C. W. Huang and K. C. Lee, "Application of ICA Technique to PCA Based Radar Target Recognition," *Progress In Electromagnetic Research*, Vol. 105, 2010, pp. 157-170.
- [25] D. Guo, X. Qu, L. Huang, and Y. Yao, "Optimized Local Superposition in Wireless Sensor Networks With T-Average-Mutual-Coherence," *Progress In Electromagnetic Research*, Vol. 122, 2012, pp. 389-411.
- [26] Z. W. Ni, M. X. Zhang, J. Li, and Q. C. Wang, "Image Compressed Sensing Based on Data-Driven Adaptive Redundant Dictionaries," *Progress In Electromagnetic Research*, Vol. 22, 2012, pp. 73-89.
- [27] B. Liu and W. Chang, "A Novel Range-Spread Target Detection Approach for Frequency Stepped Chirp Radar," *Progress In Electromagnetic Research*, Vol. 131, 2012, pp. 275-292.
- [28] Tomasz Kacmajor and Jerzy J. Michalski, "Filter Tuning Based on Linear Decomposition of Scattering Characteristics," *Progress In Electromagnetic Research*, Vol. 135, 2013, pp. 451-464.
- [29] Y. N. You, H. P. Xu, C. S. Li, and L. Q. Zhang, "Data Acquisition and Processing of Parallel Frequency SAR Based on Compressive Sensing," *Progress In Electromagnetic Research*, Vol. 133, 2013, pp. 199-215.
- [30] S. Li, Y. Tian, G. Lu, Y. Zhang, H. Xue, J. Wang, and X. Jing, "A New Kind of Non-Acoustic Speech Acquisition Method Based on Millimeter Wave Radar," *Progress In Electromagnetic Research*, Vol. 130, 2012, pp. 17-40.